AIAA JOURNAL
Vol. 50, No. 5, May 2012

Piezoelectric-Based Vibration Reduction of Turbomachinery Bladed Disks via Resonance Frequency Detuning

Jeffrey L. Kauffman* and George A. Lesieutre†
Pennsylvania State University, University Park, Pennsylvania 16802

DOI: 10.2514/1.J051344

Piezoelectric-based resonance frequency detuning can alleviate unwanted vibration of turbomachinery blades, thus reducing the dangers of high-cycle fatigue while also decreasing the blade weight. This semiactive approach applies to structures that are subjected to frequency-sweep excitation and involves altering the structural stiffness (here, by switching the piezoelectric electrical boundary conditions) to avoid a resonant condition, thus limiting the blade response. Detuning requires two switches per resonance/excitation frequency crossing, including a switch back to the original the original state, many fewer than other semiactive approaches that require four switches per cycle of vibration. Resonance frequency detuning applies to any mode of vibration with a positive electromechanical coupling coefficient, and it provides the greatest normalized vibration reduction for slow sweeps, low damping, and high coupling coefficient. Yet even for a moderate sweep rate $\alpha = 10^{-4}$ and modal damping $\zeta = 0.1\%$, optimally detuning a structure with an electromechanical coupling coefficient $k^2 = 10\%$ provides the same vibration reduction as increasing either the sweep rate or modal damping by an order of magnitude. With a lower sweep rate $\alpha = 10^{-5}$ and modal damping $\zeta = 0.01\%$, detuning with a coupling coefficient of only $k^2 = 3\%$ provides equivalent vibration reduction as an order of magnitude increase in sweep rate or modal damping.

Downloaded by PURDUE UNIVERSITY on March 4, 2013 | http://arc.aiaa.org | DOI: 10.2514/1.J051344

Nomenclature

C	=	damping matrix terms
c	=	elastic coefficients
D	=	electric displacement
E	=	electric field
F	=	generalized forces
K	=	stiffness matrix terms
k	=	electromechanical coupling coefficient
M	=	mass matrix terms
Q	=	nondimensional piezoelectric charge displacement (scaled by blocked static charge displacement)
q	=	electromechanical coupling
S	=	mechanical strain
T	=	mechanical stress
t	=	nondimensional time (scaled by structural open-circuit natural frequency)
V	=	nondimensional piezoelectric voltage (scaled by blocked static voltage)
w	=	generalized coordinates
x	=	nondimensional structural displacement (scaled by open-circuit static displacement)
α	=	linear frequency-sweep rate
ϵ	=	dielectric permittivity
ζ	=	modal mechanical damping ratio
ϕ	=	phase of excitation
ψ	=	constant part of phase of excitation
Ω	=	blade rotation speed
ω	=	frequency

Subscripts

c	=	coupled electromechanical terms
e	=	electrical terms
g	=	rotation-dependent terms
m	=	mechanical terms
oc	=	open-circuit condition
sc	=	short-circuit condition
0	=	initial value

Superscripts

D	=	constant electric displacement condition
S	=	constant strain condition
t	=	transpose operator

I. Introduction

TURBOMACHINERY has been redesigned in recent years to increase aerodynamic efficiency while decreasing drag, weight, and complexity. However, these advances have also severely decreased the damping typically intrinsic to turbomachinery blades, leaving them susceptible to high-cycle fatigue due to large vibratory stresses [1]. Beyond an extended lifetime, a reduction of the blade vibration could also allow a reduction in blade thickness, which in turn would further reduce the blade weight.

Turbomachinery blades have changing resonance frequencies due to the very large centrifugal loads they experience. Furthermore, they are subjected to excitation frequencies that are multiples of, and therefore vary with, the blade rotation speed. This excitation arises as a blade passes each of N stator vanes, producing an excitation frequency of N times that of the blade rotation. These changing resonance and excitation frequencies are often conveniently plotted together in a Campbell diagram, shown in Fig. 1. The crossing of the lines indicates where the blades will be excited resonantly, leading to large vibration amplitudes.

Most passive piezoelectric-based vibration damping methods use a shunt circuit narrowly tuned to a small set of excitation conditions. While acceptable for many structures, these techniques are inadequate for application to structures with changing dynamics subjected to multiple or changing excitation conditions, such as turbomachinery bladed disks. Although powered control systems can usually provide the needed vibration reduction under such

Presented as Paper 2011-2003 at the 19th AIAA/ASME/AHS Adaptive Structures Conference, Denver, CO, 4–7 April 2011; received 14 May 2011; revision received 28 September 2011; accepted for publication 18 October 2011. Copyright © 2012 by Jeffrey L. Kauffman and George A. Lesieutre. Published by the American Institute of Aeronautics and Astronautics, Inc., with permission. Copies of this paper may be made for personal or internal use, on condition that the copier pay the $10.00 per-copy fee to the Copyright Clearance Center, Inc., 222 Rosewood Drive, Danvers, MA 01923; include the code 0001-1452/12 and $10.00 in correspondence with the CCC.

*Ph.D. Candidate, Department of Aerospace Engineering, 229 Hammond Building. Student Member AIAA.

†Professor and Head, Department of Aerospace Engineering, 229 Hammond Building. Fellow AIAA.

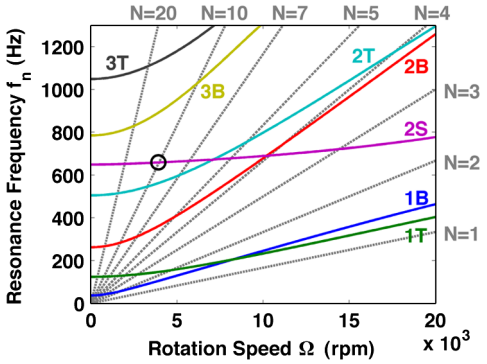

Fig. 1 Campbell diagram: natural frequencies (solid lines) and speed lines (dashed lines) with engine orders.

conditions, they are essentially isolated from a sufficiently large power source when located within the rotating frame of turbomachinery.

A vibration reduction system that can operate within the rotating frame and still apply to a wide range of vibration frequencies is desirable. Such an approach is presented here, in which a structure containing piezoelectric material is altered to detune its structural resonance frequency from that of the varying excitation. Consider, for example, an excitation associated with engine order $N = 10$, as depicted in Fig. 2a. As the rotation speed increases and the excitation frequency nears the resonance frequency of the structure, the stiffness is altered to another state, thus avoiding a resonantlike response (from $2S_1$ to $2S_0$ near 3940 rpm in Fig. 2a). When the excitation frequency has passed this excitation/resonance crossing, the stiffness can be returned to its initial state in anticipation of subsequent crossings; this returning switch also preserves the designed structural stiffness away from resonance. As presented here, this switching is implemented through the piezoelectric material: a change in its electrical boundary conditions changes the mechanical stiffness of the material, and thus the entire structure.

Figure 2 also depicts a frequency-domain understanding of detuning. With two stiffness states, there are two frequency response curves from which to choose. The idea behind detuning is to choose the lower response level. As such, for an increasing frequency sweep, the structure would begin in the stiffer open-circuit state (OC) and switch to the softer short-circuit state (SC) at the point circled in Fig. 2b. However, a key assumption in this frequency-domain analysis is harmonic motion, a simplification that is inherently violated by the swept frequency excitation. For very slow sweeps, this analysis may hold; it is expected, however, that a transient vibration analysis is required for most sweeps of interest. Such an analysis is presented here for a nominal structure containing piezoelectric material subjected to an excitation with linearly varying frequency. This analysis is carried out using nondimensional parameters to describe the system. Where numerical studies are performed, a range of parameters appropriate for turbomachinery blade operation is selected.

Note that this analysis applies to a single blade of a turbomachinery disk. In reality, blade dynamics are coupled, typically with slight mistuning (variations in physical properties) between blades that causes vibration localization [2]. As such, it is expected that resonance frequency detuning will be implemented independently on each blade; that is, separate blades will not, in general, switch stiffness states simultaneously. The act of detuning will introduce some additional stiffness mistuning between blades, although for only a very short time until the excitation/resonance condition has been passed. The duration of an altered stiffness state could be prolonged however: for example, as an intentional mistuning that may result in less blade vibration than random mistuning as described by Castanier and Pierre [3] or Hou and Cross [4].

II. Background

Resonance frequency detuning provides vibration reduction by altering the stiffness of a structure to avoid a resonant excitation condition. While any stiffness state-switching mechanism could be considered, piezoelectric material is especially attractive for the ease with which its stiffness states can be realized. Furthermore, resonance frequency detuning does not explicitly preclude the use of other vibration reduction techniques; in fact, both detuning and other piezoelectric-based approaches could conceivably use the same material, although perhaps not simultaneously.

A. Piezoelectricity

Piezoelectric material has coupled electrical and mechanical behavior that can be represented in several constitutive forms, each of which employs its own coupling terms. The linear relations in stress-field form are [5]

$$\begin{Bmatrix} T \\ E \end{Bmatrix} = \begin{bmatrix} c^D & -q^t \\ -q & (\epsilon^S)^{-1} \end{bmatrix} \begin{Bmatrix} S \\ D \end{Bmatrix} \tag{1}$$

A more important term is the electromechanical coupling coefficient k, which provides a measure of the material's ability to convert energy in each mode. Its square is the ratio of converted energy to the total work imposed on the material. Furthermore, this definition extends to a complete structure containing piezoelectric material and is defined for each mode of vibration. A convenient form of the coefficient depends only on the short- and open-circuit natural frequencies; they are readily obtained experimentally via the electrical boundary conditions and analytically through the solution to two eigenvalue problems:

$$k^2 = \frac{q^t \epsilon^S q}{c^D} = \frac{\omega_{oc}^2 - \omega_{sc}^2}{\omega_{oc}^2} \tag{2}$$

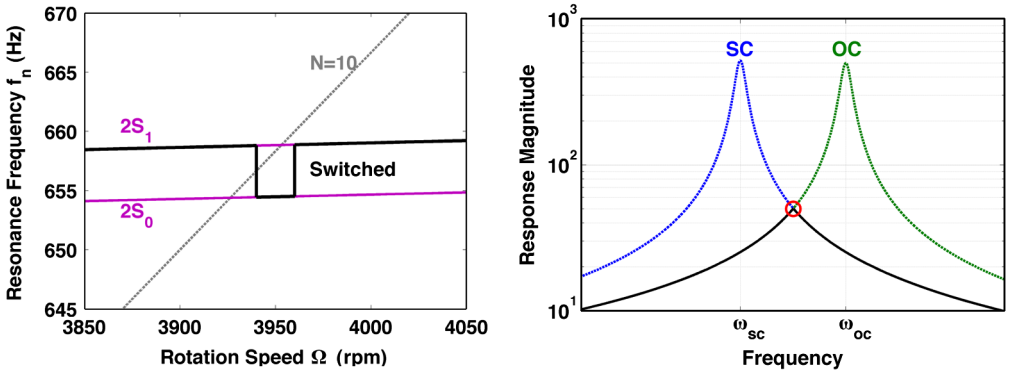

a) b)

Fig. 2 Resonance frequency detuning concept: a) two stiffness states ($2S_0$ and $2S_1$) with detuned stiffness (solid black line), and b) short-circuit (SC) and open-circuit (OC) frequency response curves (dashed lines) and optimal response (solid line).

Downloaded by PURDUE UNIVERSITY on March 4, 2013 | http://arc.aiaa.org | DOI: 10.2514/1.J051344

Downloaded by PURDUE UNIVERSITY on March 4, 2013 | http://arc.aiaa.org | DOI: 10.2514/1.J051344

B. Passive Piezoelectric-Based Vibration Reduction

A common method for exploiting the coupled electromechanical properties is to shunt piezoelectric material with a passive circuit element. This shunt changes the structural dynamics, thus altering the vibration response. Hagood and von Flotow provided a thorough treatment of a resistive shunt [6]. In this approach, the piezoelectric material converts a portion of the strain energy of the structure to electrical energy. The resistor dissipates this electrical energy as heat, thus removing energy from the system and providing damping. The performance is strongly frequency-dependent through the tuning of the circuit resistance.

Although initially examined experimentally by Forward [7], Hagood and von Flotow [6] also provided the first analytical discussion of a resonant inductive shunt, interpreting the circuit as an electrical analog to a mechanical dynamic vibration absorber . In this case, the electrical energy from the piezoelectric material moves into the resonant shunt circuit. As with the resistive shunt, optimal performance requires tuning the circuit to the desired vibration; in this case, the inductor must be tightly tuned to the frequency of vibration and the resistor modulates the bandwidth of the shunt. Yu and Wang extended this concept to a bladed disk, using a coupling capacitance to form a network of piezoelectric material and shunt circuits [8]. This piezoelectric network approach provides greater vibration reduction for mistuned structures than using individual, nominally identical shunt circuits on each blade.

Ideally, a vibration reduction system would work for multiple (or even changing) vibration frequencies. One way to extend the techniques is to include a dedicated piezoelectric material and shunt circuit for each target frequency, although this approach quickly becomes complex and unrealistic [9]. A more desirable approach is to use several shunt circuits with a single piece of piezoelectric material. Edberg et al. investigated this approach experimentally and found that the shunts required concurrent tuning [10]. Recognizing the difficulty of coupled tuning of all shunt circuits, Wu proposed adding blocking circuits to each branch [11]. These circuits, essentially band-stop filters, prevented each branch from influencing the performance of the remaining branches. Behrens and Moheimani took a similar but dramatically simpler approach, using a single current flowing circuit on each branch: essentially bandpass filters [12].

In addition to resistive and resonant inductive shunts, capacitive shunts can also be of use in vibration reduction systems. Although they do not provide inherent damping, capacitive shunts do change the system dynamics by altering the piezoelectric material stiffness, within the bounds of the short- and open-circuit stiffnesses. Davis and Lesieutre used multiple capacitances to adaptively tune a resonant shunt to a changing frequency [13]. This sort of tuning could be used to track the changing frequency due to changes in the blade rotation speed or even to avoid a resonant response at a particular frequency by moving the resonance frequency away from that of the excitation.

C. Semiactive Piezoelectric-Based Vibration Damping

Because of the complexity required to implement a passive system targeting multiple modes, a tunable, semiactive approach is more likely to be embedded in a turbomachinery blade. Common semiactive approaches involve switching the state of the piezoelectric material in a manner that reduces vibrations. Clark proposed a state-switching concept that opens (stiffens) the material when the structure is moving away from the static equilibrium position and shorts (softens) it on the return to equilibrium [14]. It thus shorts the material at peak strain energy, removing some of the stored mechanical energy and reducing the corresponding vibration.

Richard et al. developed a similar approach termed "synchronized switched damping" (SSD) [15]. Instead of shorting the material for the entire return to the equilibrium position, this approach shorts it only long enough for the charge to dissipate before returning it to the open-circuit state. With an ideally instantaneous switch, this method removes twice as much energy from the mechanical domain as Corr and Clark's technique [16].

Richard et al. enhanced the vibration reduction by switching on an inductor, inverting the piezoelectric voltage [17]. This inductor can be quite small compared with that of a resonant resistive–inductive shunt; however, it must be large enough so that the inversion occurs slowly compared with the switch duration. Lefeuvre et al. [18] and Badel et al. [19] furthered this line of techniques by switching on a voltage source. Of course, the voltage source requires significantly more power and is perhaps better classified as an active approach.

These semiactive approaches work well for multiple modes and have relatively low complexity, at least compared with a network of passive shunts for vibration reduction. Inductor-based approaches may be too large to embed in a turbomachinery blade; certainly, those requiring large amounts of power are prohibitive in the rotating frame. A key drawback of these state-switching approaches is the need for onblade sensing of the peak deflection (piezoelectric voltage) and rapid switching between shunts. Any delay in the peak detection and switching mechanisms can significantly degrade the vibration reduction performance. Furthermore, each of the above techniques switch four times per vibration cycle; at high frequencies in particular, this constraint can require large amounts of power, although self-powered systems have been developed with some added complexity.

Finally, these approaches are largely considered for implementation with a single patch of piezoelectric material. With multiple patches targeting multiple vibration modes, separate circuits will, in general, be needed for each patch for maximum vibration reduction. Some approaches (e.g., SSD) require that two patches can switch together only if they share the same compression or tension state; sharing a peak detection circuit further assumes the entire blade displaces together. While it is possible to strategically place the material with common tension or compression states for a few modes, it is almost certainly impossible to do so for all targeted modes of vibration.

III. Dynamics Model

A proper analysis of the resonance frequency detuning concept must exist in the time domain. As such, a dynamics model is ideal for direct integration of the structure's equations of motion. Because the detuning concept makes use of only short- and open-circuit electrical boundary conditions, only these limiting cases are required. However, it is instructive to begin from a full model to demonstrate how the various properties of the system combine to form the relevant nondimensional parameters.

A low-order model of the turbomachinery blade and coupled piezoelectric material dynamics provides an analytical tool to rapidly design and simulate the performance of a particular vibration reduction system. Used here is a model previously developed using the assumed modes method [20,21]. The blade displacement is written as a weighted sum of assumed shapes, with the weights providing the generalized coordinates of the system. A computation of the energy of the blade ultimately results in a set of discretized equations of motion:

$$\begin{bmatrix} M_m & 0 \\ 0 & 0 \end{bmatrix} \begin{Bmatrix} \ddot{w}_m \\ \ddot{w}_e \end{Bmatrix} + \begin{bmatrix} C_m & 0 \\ 0 & 0 \end{bmatrix} \begin{Bmatrix} \dot{w}_m \\ \dot{w}_e \end{Bmatrix} + \begin{bmatrix} K_m + \Omega^2 K_g & -K_c^t \\ -K_c & K_e^{-1} \end{bmatrix} \begin{Bmatrix} w_m \\ w_e \end{Bmatrix} = \begin{Bmatrix} F_m \\ F_e \end{Bmatrix} \tag{3}$$

Because of the rotating nature of the turbomachinery, the dynamics depend explicitly on the rotation speed Ω. An accurate representation of this dependence is necessary when designing an appropriate vibration reduction treatment, particularly in light of changing excitation frequencies, as indicated in Fig. 1. For example, piezoelectric-based passive shunts target specific resonance frequencies for vibration reduction; perhaps more important, the centrifugal loads associated with rotation can alter the mode shapes. As such, the piezoelectric material may be located in a region of high modal strain for some rotation speeds but not others, leading to a

Downloaded by PURDUE UNIVERSITY on March 4, 2013 | http://arc.aiaa.org | DOI: 10.2514/1.J051344

rotation-dependent coupling coefficient. Furthermore, there remains a possibility that the membrane loads the centrifugal loads induce may alter the effective piezoelectric properties. Finally, note that the equations of motion of the attached system, such as a shunt circuit, can be directly incorporated into Eq. (3) using the generalized coordinates and forces (for example, by writing the shunt governing equation in terms of F_e and w_e).

As a second-order dynamical system, key information about the system modes derive from the solution to the eigenvalue problem. The eigenvalues provide the natural frequencies; the eigenvectors are the assumed shape weights required to form the system mode shapes. Recalling the electromechanical coupling of Eq. (1), the piezoelectric material will provide the greatest performance if it is placed in a region of high strain, a key result of the mode shape determination.

Finally, piezoelectric material has two special electrical boundary conditions: short and open circuits. As indicated in Eq. (2), natural frequencies in these two cases form the important modal coupling coefficient, a key metric used to predict the vibration reduction potential in that particular mode for a given piezoelectric material, size, shape, and location. Note also that these electrical boundary conditions are readily produced experimentally, allowing for several points of comparison between the model predictions and experimental data.

The full form of Eq. (3) can have many parameters, so an initial simplified analysis is preferred. A first step is to define the forcing function; here, a swept sinusoidal frequency excitation of constant magnitude represents the aerodynamic loading due to rotor–stator passes [22]. Then, restricting the quantities in Eq. (3) to scalars produces nine free parameters (including several that may vary with time). Two parameters may be eliminated by assuming the spin-stiffening or -softening does not vary in time and incorporating it into the mechanical stiffness; that is, $\Omega^2 K_g$ is constant. A nondimensional form can further reduce this complexity: scaling the time by the open-circuit natural frequency, the mechanical generalized coordinate by its open-circuit static quantity, and the electrical generalized coordinate and force by their blocked static quantities reduces the number of parameters to three (the modal mechanical damping ratio ζ, the electromechanical coupling coefficient k, and the phase of the excitation ϕ):

$$\begin{aligned} \ddot{x} + 2\zeta\dot{x} + x - Q &= \sin\phi(t) \\ -k^2 x + Q &= V \end{aligned} \tag{4}$$

The phase of the excitation depends on the desired frequency sweep and can contain multiple parameters. The instantaneous frequency is the time derivative of the phase:

$$\omega(t) = \frac{\mathrm{d}\phi(t)}{\mathrm{d}t} \tag{5}$$

so the required phase of excitation is found by integrating the desired frequency sweep [23]. For a linear sweep $\omega(t) = \alpha_0 + \alpha t$,

$$\phi(t) = \int_{t_0}^{t} \omega(\tau)\,\mathrm{d}\tau = \alpha_0 t + \frac{\alpha}{2}t^2 + \underbrace{\left(-\alpha_0 t_0 - \frac{\alpha}{2}t_0^2\right)}_{\psi} \tag{6}$$

For simplicity, the constant part of the phase is often assumed as zero ($\psi = 0$, equivalent to taking $t_0 = 0$). Furthermore, sweeps are considered with zero initial frequency at time $t = 0$ so that $\alpha_0 = 0$; that is, the instantaneous frequency is $\omega = \alpha t$. Thus, the third free parameter is the linear frequency-sweep rate α.

The sweep rate can be written in terms of the dimensional linear frequency-sweep rate f_{rate} and the open-circuit natural frequency of the mode of interest f_n:

$$\alpha = \frac{f_{\text{rate}}}{2\pi f_n^2} \tag{7}$$

An upper limit on α can be estimated for typical turbomachinery by considering rapid sweep rates exciting low-frequency modes. For example, a sweep rate of 50 Hz/s (corresponding to a rotation sweep rate of 3000 rpm/s) exciting a mode at 100 Hz yields $\alpha \approx 10^{-3}$; exciting a mode at 1000 Hz yields $\alpha \approx 10^{-5}$. Certainly, higher engine order excitation (e.g., $N = 10$ as in Fig. 1) will increase the sweep rate by up to approximately an order of magnitude. In practice, however, slower rotation sweep rates are expected to excite modes with considerably higher frequencies, leading to values of α that are several orders of magnitude lower.

A sample response using this nondimensional form is shown in Fig. 3. With a sweep rate of $\alpha = 10^{-3}$ and a mechanical modal damping ratio of $\zeta = 0.1\%$, it is clear the transient response differs from that obtained by a harmonic analysis. The peak transient response level is approximately 50, an order of magnitude lower than expected from a harmonic analysis (where the peak response is approximately $1/2/\zeta = 500$). A second result is that the point of maximum dynamic amplification occurs after the excitation frequency passes the resonance frequency, as seen in Fig. 3b. These results are by no means new; however, they are important when designing a vibration reduction system for a structure subjected to a rapidly varying excitation.

The equations of motion are readily reduced to a single mechanical equation of motion in the two special cases of short and open circuits. With an open-circuit condition, $Q = 0$, and the governing equation is

$$\ddot{x} + 2\zeta\dot{x} + x = \sin\phi(t) \tag{8}$$

In the case of a short-circuit condition, $V = 0$, so Eq. (4) can be written as

$$\ddot{x} + 2\zeta\dot{x} + (1 - k^2)x = \sin\phi(t) \tag{9}$$

These equations illustrate the role of the piezoelectric material in altering the stiffness: a larger coupling coefficient k^2 results in a larger separation between the two stiffness states, and thus greater vibration reduction is expected. The solutions to the eigenvalue problems associated with Eqs. (8) and (9) also confirm Eq. (2).

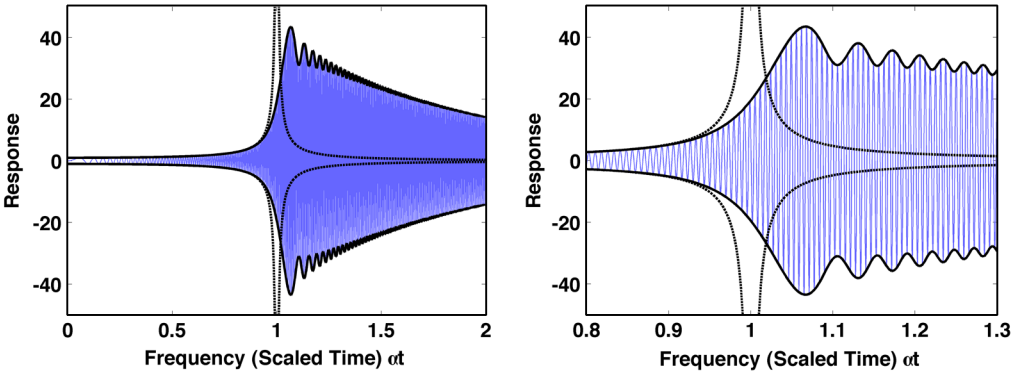

a) Full time response **b) Zoomed time response**

Fig. 3 Transient response (thin solid lines) and envelope (solid line) with steady-state response envelope (dashed line).

Downloaded by PURDUE UNIVERSITY on March 4, 2013 | http://arc.aiaa.org | DOI: 10.2514/1.J051344

The use of Eqs. (8) and (9) is governed by a switching law:

$$\begin{cases} \text{short circuit} & \omega > \omega_{\text{switch}} \\ \text{open circuit} & \omega \leq \omega_{\text{switch}} \end{cases} \tag{10}$$

From a frequency-based analysis, this optimal critical frequency ω_{switch} is the point where the short- and open-circuit frequency response functions intersect, circled in Fig. 2b:

$$\omega_{\text{switch}} = \sqrt{1 - \frac{k^2}{2}} \tag{11}$$

However, this critical frequency ω_{switch} at which the stiffness state switches may depend on several factors. Neglecting the spin-stiffening and -softening dynamics, the sweep rate (both magnitude and sign), inherent mechanical damping, and electromechanical coupling coefficient are the three free parameters of the system and may influence the optimal switch trigger.

Detuning can be simulated by time integration of the appropriate equation of motion, but this approach is very computationally intensive for low sweep rates. Ultimately, the metric of performance comparison used here is the absolute peak response. As such, actual oscillatory behavior is relatively unimportant, at least compared with the envelope of these oscillations. Thus, an approximation of the response envelope as developed by Markert and Seidler [24] is employed to significantly reduce computational complexity; alternatively, Henson provides an approximation of the vibratory response without directly integrating the equations of motion [25]. These approaches do introduce some error; with the Markert and Seidler approach [24], for example, the approximation overpredicts the peak response and shifts the time at which it occurs. These shifts (typically only a few percent) are displayed in Fig. 4. However, this error is consistent and does allow an evaluation of potential switch triggers. A particularly useful aspect of the approximation is that it accommodates a slowly changing resonance frequency (e.g., spin-stiffening and-softening), incorporating it into an effective excitation frequency-sweep rate.

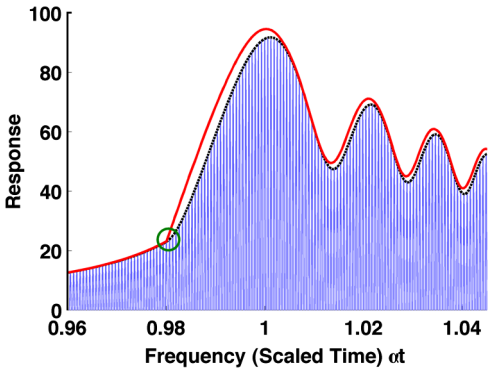

Fig. 4 Response envelopes obtained via approximation (solid line) and direct numerical integration (dashed line) for detuning at $\alpha t = 0.98$.

IV. Model Simulations and Experimental Data

A. Model Simulations

A key part of resonance frequency detuning is to switch stiffness states at the correct (optimal) time. Switching too late essentially maintains the open-circuit response (for an increasing sweep) and can even increase the blade vibration. Switching too soon can result in large dynamic amplification associated with the short-circuit resonance. This variation in response level and need for an optimal switch trigger is shown in Fig. 5. With a modal damping ratio of $\zeta = 0.1\%$, an electromechanical coupling coefficient of $k^2 = 4\%$, and a frequency-sweep ratio of $\alpha = 10^{-4}$, the structure begins in the stiffened open-circuit state. At a specific switch trigger, the structure is switched to its short-circuit state. A number of such triggers is considered; the one that produces the lowest peak response level is determined to be optimal and can be found for any combination of sweep rate, damping ratio, and coupling coefficient. This optimal trigger $(\alpha t)^* = 0.991$ is found in Fig. 5b by the minimum of the peak response level curve; the corresponding response is shown in Fig. 5a.

The optimal switch trigger can, in general, depend on the sweep rate, modal damping, and coupling coefficient; however, Fig. 6 indicates that it is primarily a function of coupling coefficient. There appears to be little difference between optimal switch triggers for a wide variety (135 in total) of sweep rate and modal damping combinations. The disparity at very low coupling can be largely ignored since it corresponds to relatively little vibration reduction: the optimal switch trigger is determined by finding the minimum peak response, and low coupling means a wide range of switch triggers provide the same vibration reduction (more accurately, the lack of vibration reduction). Some additional straying points arise similarly due to little vibration reduction for very rapid sweeps. Regardless, any variation with sweep rate and modal damping is small. Note, however, that the curves are close to but not exactly the optimal switch trigger expected from a frequency-domain analysis, as in Eq. (11). Instead, the trigger is slightly higher in frequency (or later in time) for these increasing frequency-sweep excitations.

The vibration reduction provided by resonance frequency detuning does vary significantly with sweep rate, modal damping, and coupling coefficient. An increase in any of these three parameters provides greater absolute vibration reduction; however, it is useful to consider the peak response normalized to that of an identical but unswitched open-circuit structure to identify the conditions that are most favorable to detuning. These effects are shown in Fig. 7 using a baseline sweep rate $\alpha = 10^{-4}$, modal damping $\zeta = 0.1\%$, and coupling coefficient $k^2 = 4.0\%$. Figure 7a shows that both high coupling and low sweep rate provide greater normalized vibration reduction. Similarly, Fig. 7b indicates that low modal damping and low sweep rate lead to better detuning performance, although not necessarily greater absolute vibration reduction. An interesting aspect of the performance is better displayed in Figs. 7c and 7d,

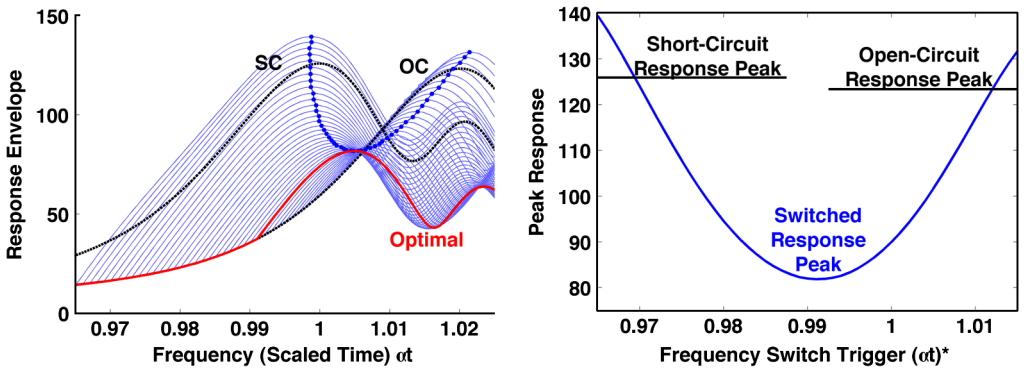

a) b)

Fig. 5 Resonance frequency detuning performance: a) response envelopes for SC, OC, and switched (thin solid lines) states, with optimal response (solid line), and b) peak response of system switched at a frequency switch trigger (αt); corresponds to dotted line in Fig. 5a.

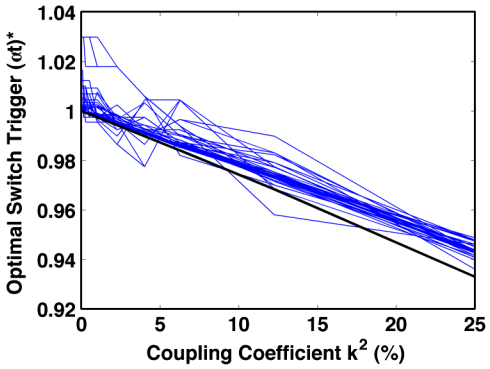

Fig. 6 Optimal switch trigger from transient (thin solid lines) and harmonic (solid line) analyses.

which show that coupling coefficient and modal damping really only play a role when the sweep rate is low enough. At higher sweep rates, the dynamic response is limited almost entirely by the rapid sweep, so the coupling coefficient and modal damping have little effect. However, these sweep rates are quite high, at least compared with those expected in turbomachinery operation. In general, detuning provides the greatest vibration reduction for structures with low modal damping subjected to low sweep rates.

While the normalized response analysis provides insight into the ideal conditions for detuning performance, it does not consider the absolute vibration level. Without detuning, the vibration could also be reduced by increasing the sweep rate or modal damping, although this approach is often difficult to implement. Nonetheless, it provides an alternative way to view the detuning performance: by considering what increase in sweep rate or modal damping is required to achieve the equivalent vibration reduction. Again using a baseline sweep rate $\alpha = 10^{-4}$ and modal damping $\zeta = 0.1\%$ (hardly ideal in light of

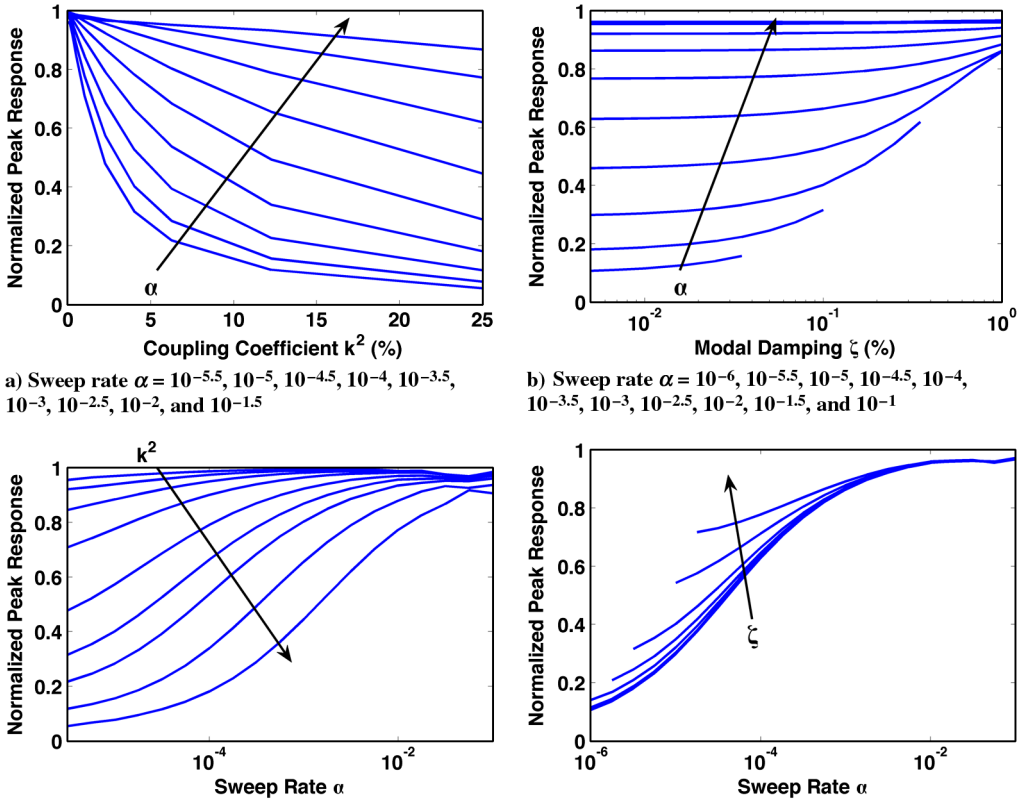

a) Sweep rate $\alpha = 10^{-5.5}, 10^{-5}, 10^{-4.5}, 10^{-4}, 10^{-3.5}, 10^{-3}, 10^{-2.5}, 10^{-2}$, and $10^{-1.5}$

b) Sweep rate $\alpha = 10^{-6}, 10^{-5.5}, 10^{-5}, 10^{-4.5}, 10^{-4}, 10^{-3.5}, 10^{-3}, 10^{-2.5}, 10^{-2}, 10^{-1.5}$, and 10^{-1}

c) Coupling coefficient $k^2 = 0.1225, 0.25, 0.49, 1, 2.25, 4, 6.25, 12.25$, and 25%

d) Modal damping $\zeta = 0.005, 0.01, 0.05, 0.1, 0.5$, and 1%

Fig. 7 Peak response (normalized by unswitched open-circuit response) of detuned structure.

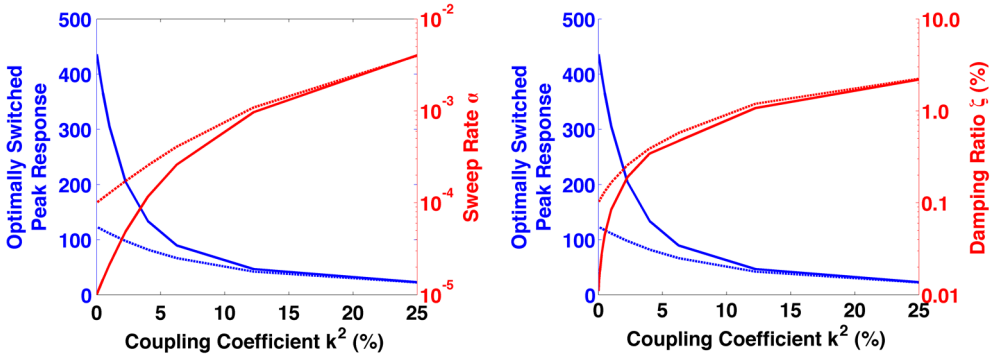

a) Required sweep rate

b) Required damping ratio

Fig. 8 Required system parameters for equivalent vibration reduction as detuning with a nominal sweep rate $\alpha = 10^{-4}$ and damping ratio $\zeta = 0.1\%$ (dashed lines) or $\alpha = 10^{-5}$ and $\zeta = 0.01\%$ (solid lines).

Downloaded by PURDUE UNIVERSITY on March 4, 2013 | http://arc.aiaa.org | DOI: 10.2514/1.J051344

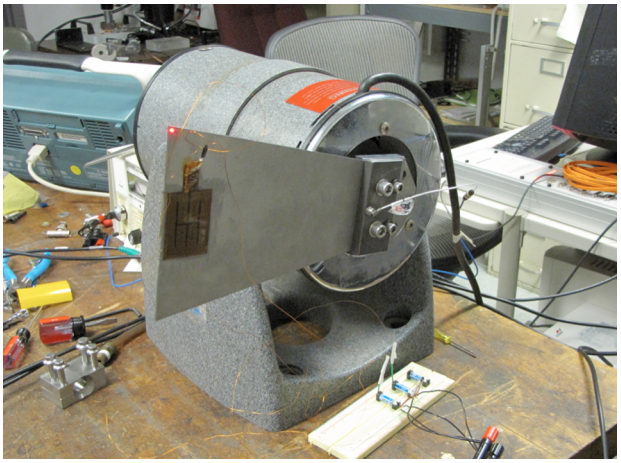

Fig. 9 Representative metallic blade with surface-mounted monolithic piezoelectric patch. Stiffness state is switched via relays in foreground.

Fig. 7), Fig. 8 shows that, even for small coupling coefficients, significant increases in sweep rate or modal damping would be required. For a moderate coupling coefficient $k^2 = 10\%$, detuning provides the same vibration reduction as increasing the sweep rate or modal damping by an order of magnitude. This effect is magnified for slower sweeps or less damping: with a sweep rate of $\alpha = 10^{-5}$ and a modal damping of $\zeta = 0.01\%$, a coupling coefficient of $k^2 = 3\%$ provides equivalent vibration reduction as an order of magnitude increase in sweep rate or modal damping.

B. Experimental Data

Blades are analyzed experimentally in the stationary frame. Figure 9 shows a representative trapezoidal titanium flat plate with surface-mounted piezoelectric material patches. For this particular plate, two Midé QP10w patches (one shown and one on the reverse side of the plate) are mounted near the plate tip. All blades are mounted with cantilever boundary conditions to the shaker armature. A dSPACE system controls the shaker in addition to capturing the blade response through a combination of accelerometer and laser vibrometer signals.

The initial experimental testing focuses on two modes of interest: the two-stripe and third bending modes have open-circuit resonance frequencies at 664.3 and 785.1 Hz and blade coupling coefficients of 0.0886 and 0.0691, respectively. Figure 10 shows the vibration reduction possible for the two-stripe mode. With a sweep rate of approximately $\alpha = 10^{-5}$ and modal damping of $\zeta = 0.08\%$, optimal switching of the piezoelectric material's electrical boundary conditions can reduce the vibration by 20%. Simulations indicate slightly larger vibration reductions are possible, although performance is sensitive to the system parameters. Because of the very low intrinsic damping of the blade, however, even small increases in effective damping can result in large vibration reductions.

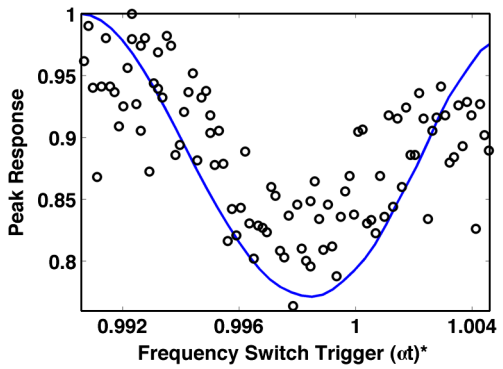

Fig. 10 Resonance frequency detuning experimental performance (circles) and simulated results (solid line) for many frequency-based switch triggers.

V. Conclusions

The ultimate goal of this research is to reduce the large vibration experienced by turbomachinery bladed disks via piezoelectric-based damping or vibration control. Analytical simulations predict and experimental data confirm that resonance frequency detuning can reduce this vibration by altering the structural stiffness to detune it from the excitation, thus avoiding a resonant response. By requiring only two switches per excitation/resonance frequency crossing, detuning is significantly less sensitive to the switching time and requires less power than typical semiactive approaches that switch multiple times per vibration cycle; more important, it may provide a more realistic implementation in turbomachinery. The timing of the detuning is important and varies primarily with the coupling coefficient, although a more general understanding of the optimal switch trigger is required before implementation. With optimal switching, the amount of dynamic amplification is governed by the system's inherent mechanical damping, the system modal electromechanical coupling coefficient, and the excitation frequency-sweep rate. Resonance frequency detuning is ideal for structures with low modal damping subjected to slow frequency-sweep excitation; however, an increase in coupling coefficient, modal damping, or sweep rate will reduce the structural response for an optimal switch trigger.

Acknowledgments

This work is supported through a NASA Graduate Student Researchers Program Fellowship (contract number NNX08AZ10H). The authors also thank the NASA John H. Glenn Research Center Active Structures Team for their insights and Kirsten Duffy and George Stefko for their advice and mentorship.

References

[1] El-Aini, Y., de Lanueuville, R., Stoner, A., and Capece, V., "High Cycle Fatigue of Turbomachinery Components: Industry Perspective," 33rd AIAA/ASME/SAE/ASEE Joint Propulsion Conference, AIAA Paper 1997-3365, 1997.

[2] Ewins, D. J., "The Effects of Detuning Upon the Forced Vibrations of Bladed Disks," *Journal of Sound and Vibration*, Vol. 9, No. 1, 1969, pp. 65–79. doi:10.1016/0022-460X(69)90264-8

[3] Castanier, M. P., and Pierre, C., "Using Intentional Mistuning in the Design of Turbomachinery Rotors," *AIAA Journal*, Vol. 40, No. 10, 2002, pp. 2077–2086. doi:10.2514/2.1542

[4] Hou, J., and Cross, C., "Minimizing Blade Dynamic Response in a Bladed Disk Through Design Optimization," *AIAA Journal*, Vol. 43, No. 2, 2005, pp. 406–412. doi:10.2514/1.11526

[5] "IEEE Standard on Piezoelectricity," IEEE Std. 176-1987, New York, 1987.

[6] Hagood, N. W., and von Flotow, A., "Damping of Structural Vibrations with Piezoelectric Materials and Passive Electrical Networks," *Journal of Sound and Vibration*, Vol. 146, No. 2, 1991, pp. 243–268. doi:10.1016/0022-460X(91)90762-9

[7] Forward, R. L., "Electronic Damping of Vibrations in Optical Structures," *Applied Optics*, Vol. 18, No. 5, 1979, pp. 690–697. doi:10.1364/AO.18.000690

[8] Yu, H., and Wang, K. W., "Piezoelectric Networks for Vibration Suppression of Mistuned Bladed Disks," *Journal of Vibration and Acoustics*, Vol. 129, No. 5, 2007, pp. 559–566. doi:10.1115/1.2775511

[9] Viana, F. A. C., and Steffen, V. Jr., "Multimodal Vibration Damping through Piezoelectric Patches and Optimal Resonant Shunt Circuits," *Journal of the Brazilian Society of Mechanical Sciences and Engineering*, Vol. 28, No. 3, 2006, pp. 293–310. doi:10.1590/S1678-58782006000300007

[10] Edberg, D. L., Bicos, A. S., Fuller, C. M., Tracy, J. J., and Fechter, J., "Theoretical and Experimental Studies of a Truss Incorporating Active Members," *Journal of Intelligent Material Systems and Structures*, Vol. 3, 1992, pp. 333–347. doi:10.1177/1045389X9200300209

[11] Wu, S.-Y., "Method for Multiple-Mode Shunt Damping of Structural Vibration Using a Single PZT Transducer," *Proceedings of the SPIE*

Downloaded by PURDUE UNIVERSITY on March 4, 2013 | http://arc.aiaa.org | DOI: 10.2514/1.J051344

Conference on Smart Structures and Materials 1998, San Diego, CA, Vol. 3327, SPIE, Bellingham, WA, 1998, pp. 159–168. doi:10.1117/12.310680

[12] Behrens, S., and Moheimani, S. O. R., "Current Flowing Multiple-mode Piezoelectric Shunt Dampener," *Proceedings of the SPIE Conference on Smart Structures and Materials 2002*, San Diego, CA, Vol. 4697, SPIE, Bellingham, WA, 2002, pp. 217–226. doi:10.1117/12.472658

[13] Davis, C. L., and Lesieutre, G. A., "An Actively Tuned Solid-State Vibration Absorber Using Capacitive Shunting of Piezoelectric Stiffness," *Journal of Sound and Vibration*, Vol. 232, No. 3, 2000, pp. 601–617. doi:10.1006/jsvi.1999.2755

[14] Clark, W. W., "Vibration Control with State-Switched Piezoelectric Materials," *Journal of Intelligent Material Systems and Structures*, Vol. 11, No. 4, 2000, pp. 263–271. doi:10.1106/18CE-77K4-DYMG-RKBB

[15] Richard, C., Guyomar, D., Audigier, D., and Ching, G., "Semi-Passive Damping Using Continuous Switching of a Piezoelectric Device," *Proceedings of the SPIE Conference on Smart Structures and Materials 1999*, Newport Beach, CA, Vol. 3672, SPIE, Bellingham, WA, 1999, pp. 104–111. doi:10.1117/12.349773

[16] Corr, L. R., and Clark, W. W., "Comparison of Low-frequency Piezoceramic Shunt Techniques for Structural Damping," *Proceedings of the SPIE Conference on Smart Materials and Structures 2001*, Newport Beach, CA, Vol. 4331, SPIE, Bellingham, WA, 2001, pp. 262–272. doi:10.1117/12.432709

[17] Richard, C., Guyomar, D., Audigier, D., and Bassaler, H., "Enhanced Semi-Passive Damping Using Continuous Switching of a Piezoelectric Device on an Inductor," *Proceedings of the SPIE Conference on Smart Structures and Materials 2000*, Newport Beach, CA, Vol. 3989, SPIE, Bellingham, WA, 2000, pp. 288–299. doi: 10.1117/12.384569

[18] Lefeuvre, E., Badel, A., Petit, L., Richard, C., and Guyomar, D., "Semi-Passive Piezoelectric Structural Damping by Synchronized Switching on Voltage Sources," *Journal of Intelligent Material Systems and Structures*, Vol. 17, Nos. 8–9, 2006, pp. 653–660. doi:10.1177/1045389X06055810

[19] Badel, A., Sebald, G., Guyomar, D., Lallart, M., Lefeuvre, E., and Richard, C., "Piezoelectric Vibration Control by Synchronized Switching on Adaptive Voltage Sources: Towards Wideband Semi-Active Damping," *Journal of the Acoustical Society of America*, Vol. 119, No. 5, 2006, pp. 2815–2825. doi:10.1121/1.2184149

[20] Kauffman, J. L., and Lesieutre, G. A., "A Low-Order Model for the Design of Piezoelectric Energy Harvesting Devices," *Journal of Intelligent Material Systems and Structures*, Vol. 20, No. 5, 2009, pp. 495–504. doi:10.1177/1045389X08101559

[21] Kauffman, J. L., and Lesieutre, G. A., "Reduction of High-Cycle Fatigue in Integrally Bladed Rotors through Piezoelectric Vibration Damping," *Proceedings of the 20th International Conference on Adaptive Structures and Technologies* [CD-ROM], Chinese Univ. of Hong Kong and Sha Tin, Hong Kong, 2009, pp. 218–229.

[22] Korakianitis, T., "Influence of Stator-Rotor Gap on Axial-Turbine Unsteady Forcing Functions," *AIAA Journal*, Vol. 31, No. 7, 1993, pp. 1256–1264. doi:10.2514/3.11761

[23] van der Pol, B., "The Fundamental Principles of Frequency Modulation," *Journal of the Institution of Electrical Engineers, Part III: Radio and Communication Engineering*, Vol. 93, No. 23, 1946, pp. 153–158. doi:10.1049/ji-3-2.1946.0024

[24] Markert, R., and Seidler, M., "Analytically Based Estimation of the Maximum Amplitude During Passage Through Resonance," *International Journal of Solids and Structures*, Vol. 38, Nos. 10–13, 2001, pp. 1975–1992. doi:10.1016/S0020-7683(00)00147-5

[25] Henson, G. M., "Response of an Oscillating System to Harmonic Forces of Time-Varying Frequency," *AIAA Journal*, Vol. 46, No. 8, 2008, pp. 2033–2041. doi:10.2514/1.34662

B. Epureanu
Associate Editor

Downloaded by PURDUE UNIVERSITY on March 4, 2013 | http://arc.aiaa.org | DOI: 10.2514/1.J051344